Mechatronics and Intelligent Transportation Systems
https://www.acadlore.com/journals/MITS

Dynamic Performance of Low- and Medium-Speed Maglev Train Running on the Turnout

Sumei Wang[1], Qi Zhu[2], Yiqing Ni[1], Junqi Xu[3*], Feng Chen[4]

[1] National Rail Transit Electrification and Automation Engineering Technology Research Center (Hong Kong Branch), 999077 Hong Kong SAR, China
[2] Department of Civil and Environmental Engineering, The Hong Kong Polytechnic University, 999077 Hong Kong SAR, China
[3] Tongji University Maglev Transportation Engineering R&D Center, 201306 Shanghai, China
[4] Hunan Rail Technology Application Research Center Co., Ltd, 410000 Changsha, China

[*] Correspondence: Junqi Xu (12120@tongji.edu.cn)

Received: 02-25-2023 **Revised:** 03-10-2023 **Accepted:** 03-17-2023

Citation: S. M. Wang, Q. Zhu, Y. Q. Ni, J. Q. Xu, and F. Chen, "Dynamic performance of low- and medium-speed maglev train running on the turnout," *Mechatron. Intell Transp. Syst.*, vol. 2, no. 1, pp. 32-41, 2023. https://doi.org/10.56578/mits020104.

Abstract: This study aimed to analyze dynamic performance of the low- and medium-speed maglev train on the turnout, by conducting a series of field tests on the Fenghuang maglev sightseeing express line. This study systematically analyzed and evaluated dynamic responses of vehicle body, suspension bogie, short rail joint, motor-driven long-span girder (LSG) and continuous beam of the turnout at different speeds and loads in time and frequency domains. Test results obtained in this study indicated that: 1) speed and load of the maglev train affected acceleration amplitude of the train and turnout; 2) vertical sperling indexes of the test train were less than 2.5, indicating that the train had good ride quality; and 3) resonance phenomenon of track occurred at 40 km/h. The findings of this study may serve as references for model validation and optimized design of low- and medium-speed maglev train.

Keywords: Low-and medium-speed maglev; Dynamic performance; Field test; Turnout

1. Introduction

Guided transport has been developed fast all over the world in the past decades due to the higher transport capacity and energy efficiency in operation compared with road traffic and air traffic. Nevertheless, conventional rail transport systems are limited by a series of technical issues related to adhesion, rail-wheel wear, noise and vibration [1]. Maglev systems come as new types of guided transport systems which have the advantages of non-contact operation, low vibration, low noise, no risk of derailment, flexible route selection and low comprehensive construction costs and thus has received widespread attention for its development and application in Japan, Korea and China [2]. Especially, low- and medium-speed maglev lines have been commercially operated, such as China's Changsha Airport Line (18.55 km), Japan's Linimo (8.9 km) and South Korea's Incheon Airport Maglev Line (6.1 km) [3].

With the operation of the maglev line, a strong coupling interaction has been shown to occur between the maglev train, suspension control and guideway systems, thus comprising a time-varying system problem. Related research has been conducted to analyze the dynamic performance of low- and medium-speed maglev system [4-8]. The interaction effect contributes an additional damping or mass effect to the vibration of the guideway, which causes temporal variations in the natural frequency and modal damping ratio of the guideway. The flexibility of the guideway, which acts as an external force of excitation on the train, may also generate dynamic instability and unacceptable vibration, such as self-excited and resonant vibrations [4, 5]. As the frequency of the external excitation acting on the train approaches the natural frequency of the train vehicles, the dynamic response of the train tends to increase significantly, resulting in resonance [6, 7]. Resonance-induced instability of the levitation gap, which can lead to failure of suspension control, has been observed in maglev trains on both test and

commercial lines. Hence, to ensure the operational stability and safety of maglev trains, it is essential to study the complicated dynamic interaction mechanism of the maglev train-suspension-guideway system.

The dynamic interaction of the maglev train-suspension-guideway system is relatively difficult to evaluate because it involves mechanics, electronics and control theory [8]. Early studies used simplified analytical models to examine the dynamic interaction of the maglev system. The guideway was also generally treated as a simple or continuous beam supported by the mode superposition method, and simplified vehicle models were developed without considering the suspension control [9-19]. Following the improved simulation of the maglev vehicle and electromagnet interaction, more complicated vehicle/guideway models such as two-dimensional [15-19] and three-dimensional vehicle models [20-22] were developed that consider the proportional-integral-derivative (PID) control [15] or LQG control theory [13]. These models have been used to investigate more complicated dynamic interactions of maglev systems including the effects of irregularities [17, 19], resonant conditions [15], ground settlement [23] and cross-wind loads [24]. Field experiments [25-31] were also conducted to investigate the dynamic response of maglev vehicles running on a bridge. The data from the field experiments subsequently enabled the established numerical model to be verified and used to predict the system response. Overall, studies have generally used model-based methods, such as simple analytical or finite element methods, to conduct numerical investigations of the dynamic responses under various conditions, with data from field experiments being used to verify the established models [32]. However, few studies have been conducted on the maglev train-turnout dynamic interactions, as most of the existing research has focused on concrete bridges typically used on main lines [33-36]. Moreover, field tests conducted on a real operational maglev line are inadequate for turnout.

The turnout is one of the most critical structures in the maglev system to enable the trafficability of the track. To ensure its switching function, the turnout is constructed of steel with very lightweight. However, compared with the normal guideway line, it is a more complex structure. Therefore, the dynamic interaction of the train and the turnout is likely to be more violent than that of train and ordinary concrete bridge, which in turn will further affect the running safety and the riding experience, posing a challenge to the solidity of the turnout. Moreover, it is difficult to characterise the dynamic features of turnout by means of the model-based method. Hence, in this paper, field tests of the Fenghuang maglev sightseeing express line are conducted to study the dynamic performance of the low- and medium-speed maglev train moving on the turnout. This study will provide basic data references for numerical model verification, scientific design, promotion of the related standards.

The reminder of the paper is arranged as follows: Section 2 has a detailed introduction to the information of test train, test line, as well as test scheme; Section 3 discusses the test results of the system's dynamic responses including vehicle body and the turnout under different operating conditions, and key dynamic index and frequency spectrum characteristics of the system are also analyzed; the relevant conclusions are given in Section 4.

2. Design of Field Test Scheme

2.1 Test Train

The maglev train (Figure 1) for the field test adopts electromagnetic suspension (EMS) guiding technique and short-stator linear induction motor traction technique. The train has one vehicle body, five suspension bogies and forty electromagnets. Each suspension bogie is decoupled into two side bogies connected by the anti-rolling beams to prevent the suspension bogies from rolling. There are four air springs between the vehicle body and each suspension bogie. The interaction between the F-type rail and the electromagnets is realised through electromagnetic forces, which are controlled by a designated PID controller. The key structural components of the suspension bogies are as shown in Figure 2, and main technical parameters of the maglev train are shown in Table 1.

Figure1. Low- and medium-speed maglev

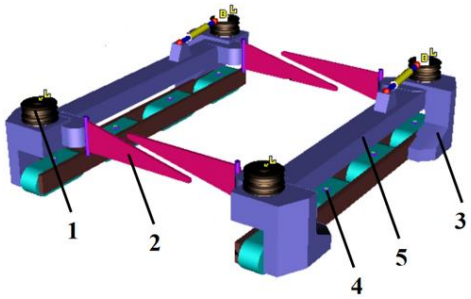

1-Air spring; 2-Anti-rolling beam; 3-Corbel; 4- Electromagnet; 5- Bracket

Figure 2. Suspension bogie

Table 1. Main technical parameters of the train [30]

Technical specification	Parameters
Train length (mm)	16500 (end), 15600 (middle)
Train width (mm)	2800
Maximum train height (mm)	≤3700
Net height inside (mm)	≥2100
Floor height (mm)	≤880
AW0 train weight (t)	≤24
Train suspension ability (t)	≥33
Suspension frame module length (mm)	≤2800
Rail gauge (mm)	1860
Centerline of coupler's height (mm)	600±5
Number of doors on each side	2
Starting acceleration (m/s^2)	≥0.9
Common braking deceleration (m/s^2)	≥1.1
Emergency braking deceleration (m/s^2)	≥1.3

2.2 Test Line

Fenghuang maglev sightseeing express line is the first "maglev + culture + tourism" project in the world. Fenghuang maglev project seamlessly connects Zhangjihuai high-speed rail with a total length of 9.121 km. It starts from Fenghuanggucheng Station of Zhangjihuai high-speed railway, passes through the Tourist Service Center in the North of the City, and finally reaches the tunnel entrance of Folklore Park in the direction of 209 Around City Line.

The Fenghuang maglev sightseeing express line includes turnouts, straight sections, small radius curve sections, slop sections and tunnel sections. The function of the turnout is to change the running route of the maglev train from one line to another by the motor-driven long-span girder (LSG). As shown in Figure 3, the turnout of the Fenghuang maglev sightseeing express line is a single joint turnout with three segments i.e., main line, auxiliary line and turnout. There is one short rail joint on the auxiliary line to connect the two F-type rail ends.

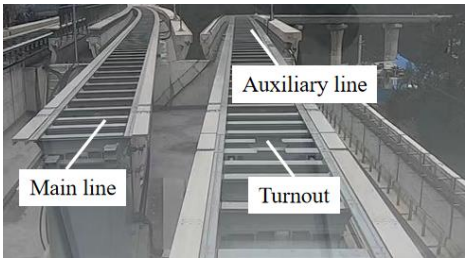

Figure 3. Turnout of the test line

2.3 Test Scheme

To explore the dynamic performance of the test maglev system when the low- and medium-speed maglev train is moving on the turnout, 18 test points are arranged on the vehicle body, suspension bogie, as well as at short rail joint, LSG and continuous beam of the turnout in total. The detailed measurement points for the train and turnout are listed in Table 2.

Furthermore, to fully test the dynamic performance of the train and turnout, different train loads are considered as AW0 (weight of an empty vehicle), AW2 (AW0+weight of seated passengers+weight of standees with 4 people/m^2), and AW3 (AW0+weight of seated passengers+weight of standees with 6 people/m^2) [37], and the test speeds are set in a 20 ~ 60 km/h range with an interval of 20 km/h to ensure the safe operation of the test train.

The sampling frequency is set as 5000 Hz, and all the data are collected by an online monitoring system installed on the moving vehicle, track and bridge.

Table 2. Measurement point location of the train and turnout

Measurement position		Location	Direction
Vehicle	Vehicle body	Left side of front end	La./Ve./Lo.
		Middle	Ve.
		Rear end	La./Ve.
	2# Suspension frame	Left side of front end	Ve.
		Left side of rear end	La./Ve./Lo.
		Right side of front end	Ve.
		Right side of rear end	La./Ve.
	3# Suspension frame	Left side of front end	La./Ve.
		Left side of rear end	Ve.
		Right side of front end	Ve.
		Right side of rear end	Ve.
Turnout	Short rail joint	F-rail	La./Ve.
	Continuous beam	Mid-span of the 2nd span	Ve.
		F-rail of the mid-span of the 2nd span	Ve.
		1/4-span of the 2nd span	Ve.
		F-rail of the 1/4-span of the 2nd span	Ve.
	LSG	1st LSG	Ve.
		F-rail of the 1st LSG	Ve.

Note: La.-Lateral, Ve.-Vertical, Lo.-Longitudinal

3. Results and Discussion

3.1 Vibration Analysis of the Train

3.1.1 Vehicle body

To investigate the impact of the running speed and the load of the test train on the vibration of vehicle body when the maglev train passes through the turnout, the maximum vertical acceleration amplitudes of the 3 measured points at the vehicle body under different operating conditions are shown in Figure 4. It can be observed that the acceleration amplitudes of the carriage at speed of 20 km/h are the smallest, while the acceleration amplitudes at speed of 40 km/h are a little larger than at other speeds at most cases. The phenomenon is much more obvious with the load condition as AW2. According to reference [32], it is known that train resonance occurs when a train is moving on a guideway at the resonance speed, it can be concluded that 40 km/h can be the resonance speed for the test system.

It is found that the acceleration of the front and middle points of the vehicle body is larger than that of the middle point due to the pitching motion of the vehicle body. The amplitude of the acceleration is within the range of 0.1772 m/s^2 and 0.512 m/s^2 at the front point, 0.1131 m/s^2 and 0.2698 m/s^2 at the middle point, and 0.2429 m/s^2 and 0.4387 m/s^2 at the rear point of the vehicle body, respectively. To further evaluate the comfort of the vehicle body, Sperling indexes (defined in GB/T 5599-2019) of the three measured points are calculated under different operating conditions. Here, the Sperling index is given by [38]:

$$W_i = 3.57\sqrt[10]{\frac{A_i^3}{f_i}F(f_i)} \tag{1}$$

where A_i is the vibration acceleration, f_i is the vibration frequency, $F(f_i)$ is the frequency correlation coefficient given in Table 3.

When the dynamic response contains multiple frequency components, the Sperling index is calculated as:

$$W = \sqrt[10]{\sum_{i=1}^{n} W_i^{10}} \tag{2}$$

Table 3. Frequency correlation coefficient

Vertical		Lateral	
0.5~5.9 Hz	$F(f)=0.325f$	0.5 ~ 5.4 Hz	$F(f)=0.8f$
5.9~20 Hz	$F(f)=400/f^2$	5.4 ~ 26 Hz	$F(f)=650/f^2$
>20 Hz	$F(f)=1$	>26 Hz	$F(f)=1$

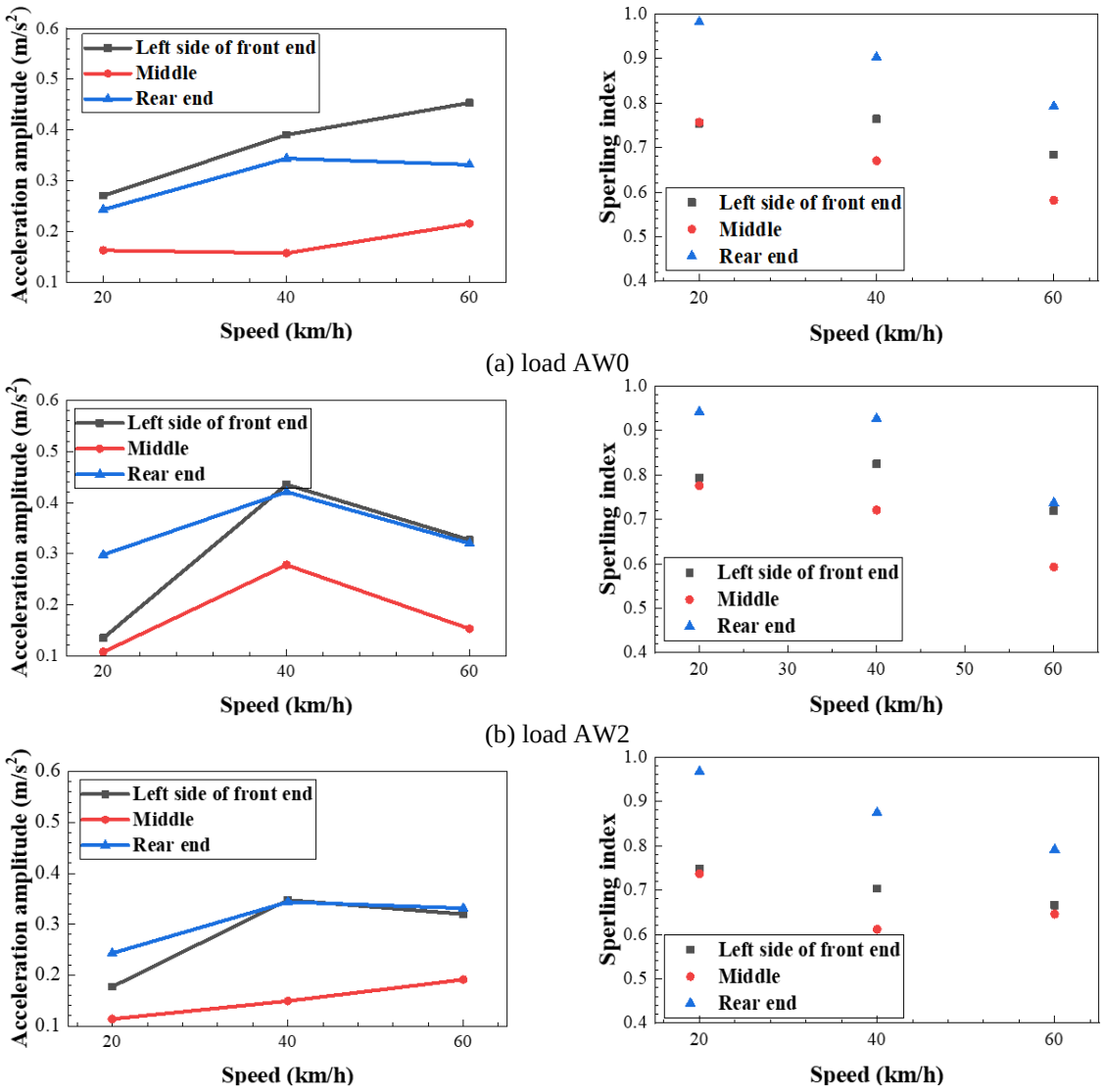

Figure 4. Maximum acceleration amplitudes and Sperling indexes of the vehicle body with different speeds and loadings

As shown in Figure 4, it can be seen that the Spering indexes of the maglev train at the location of front and rear are higher than these at the location of middle. All the Spring indexes of the maglev train are lower than 1, which indicates the stability of the maglev train is excellent since all the indexes do not exceed 2.5. Moreover, the train speed and loading have little effect on the comfort of the maglev train.

3.1.2 Suspension bogie

The dynamic performance of the suspension bogie is also investigated when the maglev train passes through the turnout. The maximum acceleration amplitudes of the measured points installed at 2# and 3# suspension frames under different operating conditions are shown in Figure 5. It is found that the acceleration amplitude of the vehicle body is much smaller than the suspension bogie due to the air spring by comparing the Figures 4 and 5. Meanwhile, as shown in Figure 5, the maximum accelerations of the suspension bogie exhibit similar patterns with the vehicle body, for which the acceleration amplitudes of the running speed as 20 km/h are the smallest basically, and the amplitudes at speed of 40 km/h is larger than the 60 km/h and 20 km/h at most cases with load condition as AW2.

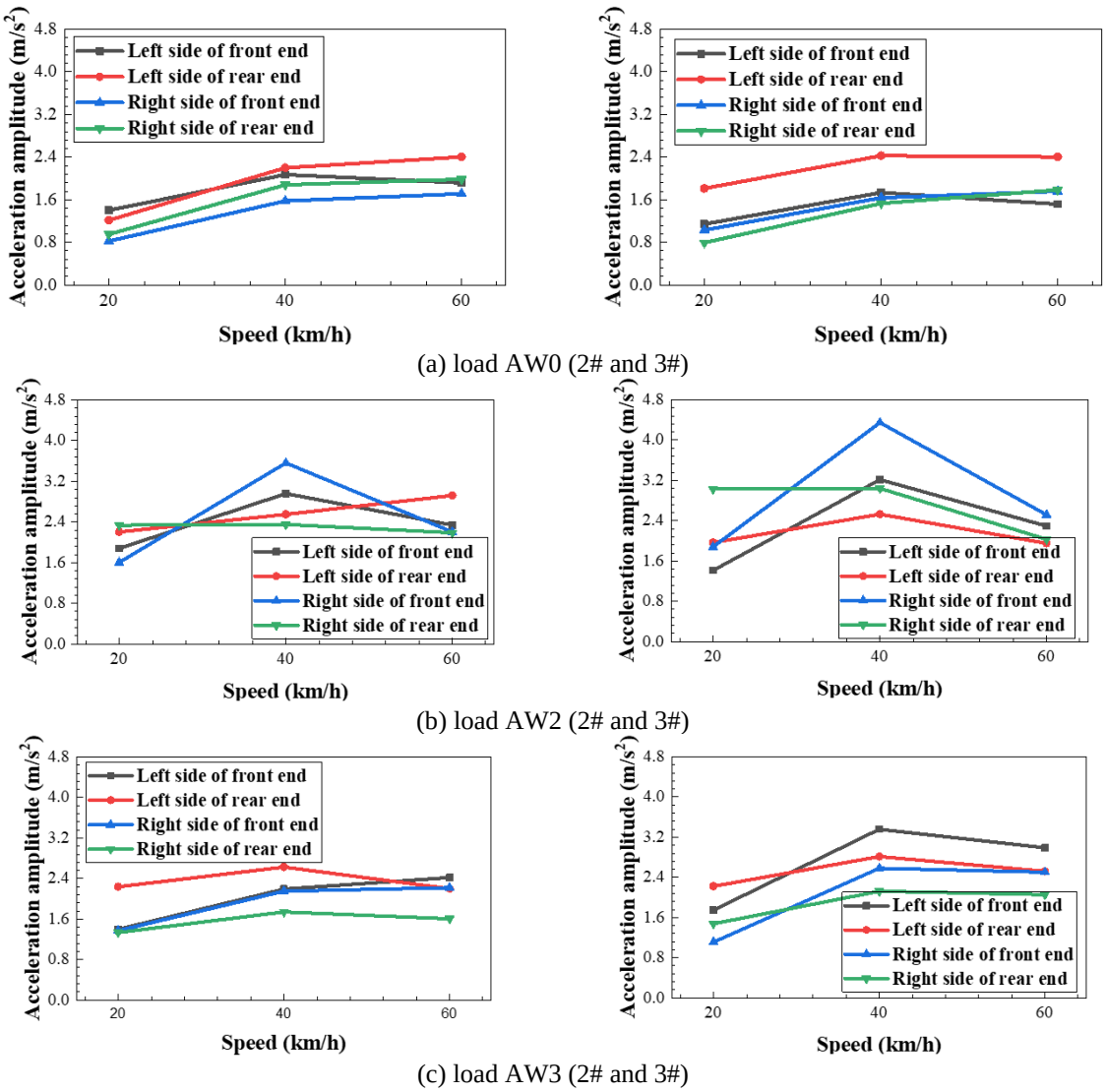

Figure 5. Maximum acceleration amplitudes of the suspension bogie with different speeds and loadings

When examing the amplitudes of the suspension frames, it is found out that the amplitudes of the accelerations for the 2# suspension frame is within the range of 1.3943 m/s^2 and 2.4205 m/s^2 for the left side of front end, 1.2158 m/s^2 and 2.9202 m/s^2 for the left side of rear end, 0.8212 m/s^2 and 3.5616 m/s^2 for the right side of front end, and 0.9514 m/s^2 and 2.3493 m/s^2 for the right side of rear end, respectively. The amplitudes of the acceleration for the 3# suspension frame are within the range of 1.1438 m/s^2 and 3.3596 m/s^2 for the left side of front end, 1.8099 m/s^2 and 2.8168 m/s^2 for the left side of rear end, 1.0294 m/s^2 and 4.3464 m/s^2 for the right side of front end, and 0.7927 m/s^2 and 3.0401 m/s^2 for the right side of rear end, respectively. The acceleration responses of the 2# and 3# suspension frames are different because they are controlled by different controllers.

3.2 Vibration Analysis of the Turnout

To further investigate the dynamic performance of turnout, the maglev train with the load as AW2 moving on the turnout is considered. The maximum acceleration amplitudes of the measured points installed on turnout under different train speeds are shown in Figure 6, and the fast Fourier Transform is performed to analyze the data in the frequency domain and plotted in Figure 7.

As seen in Figure 6, it can be observed that theacceleration amplitudes of the F-rail on the short rail joint and the continuous beam come to be largest when the train speed is up to 40 km/h, which is consistent with the phenomenon observed from Figure 4 and Figure 5. It can be obviously observed from Figure 7 that the resonance occurs at speed of 40 km/h with the resonance frequency being 24.2 Hz. The acceleration of the F-rail on the continuous beam is shown in Figure 8, and the resonance phenomena can also be obviously observed from time domain in the figure. It can also explain the larger acceleration amplitudes of the vehicle at speed of 40 km/h under such operation condition.

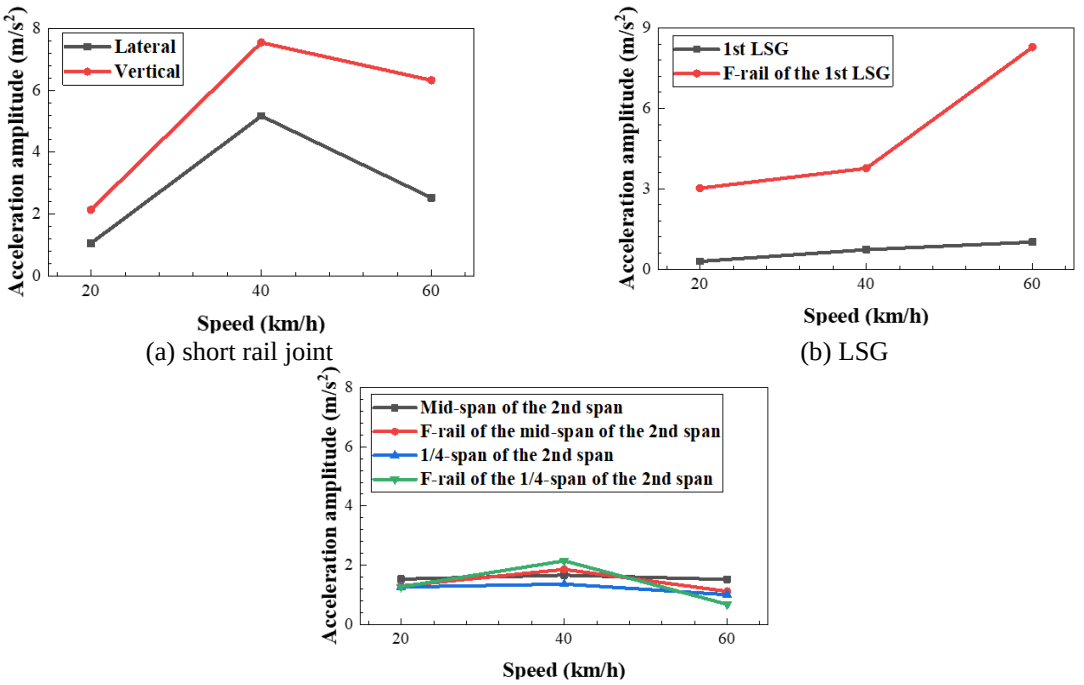

Figure 6. Acceleration of the turnout at different speeds

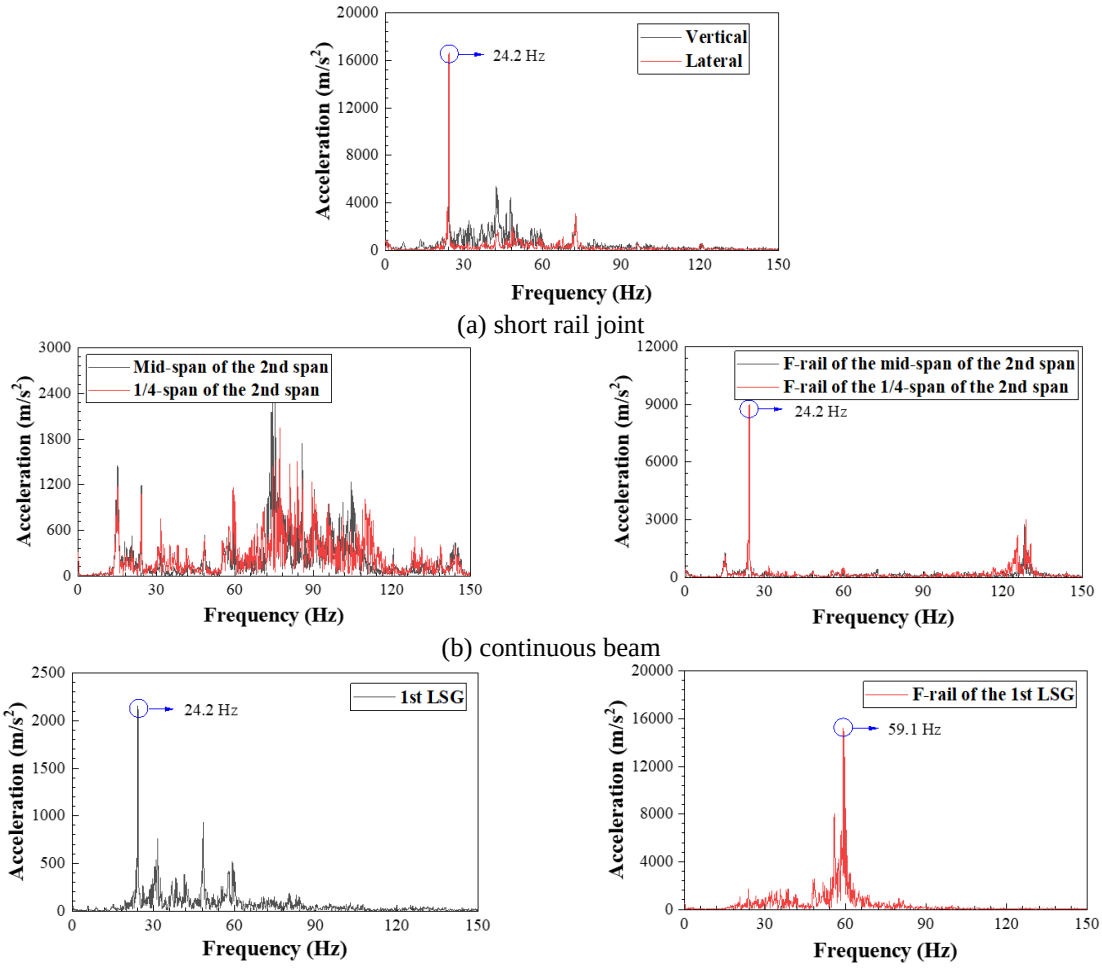

Figure 7. Frequency of the turnout at speed of 40 km/h

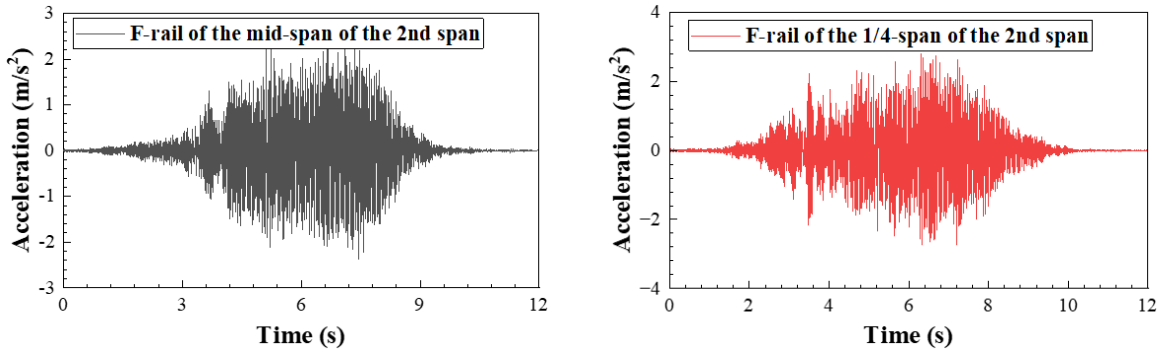

Figure 8. Acceleration of the turnout at speed of 40 km/h

In addition, the amplitudes of the acceleration for the short rail joint are within the range of 1.0499 m/s^2 and 5.1689 m/s^2 for lateral, and between 2.1305 m/s^2 and 7.5462 m/s^2 for vertical. As for the continuous beam, the amplitudes are within 1.0021 m/s^2 and 1.6603 m/s^2 for beam, and within 0.6746 m/s^2 and 2.1425 m/s^2 for the F-rail. For the LSG, they are within 0.2899 m/s^2 and 1.0093 m/s^2 for the beam, and between 3.0192 m/s^2 and 8.2872 m/s^2 for the F-rail. It can be concluded that the amplitude of the F-rail is larger than the bridge due to the steel sleepers which function as springs.

4. Conclusion

Experimental study is conducted on the Fenghuang maglev sightseeing express line, and dynamic performance of the maglev train passing through the turnout section is analyzed in detail in both time and frequency domains. The main conclusions are listed below:

(1) The speed and load of the maglev train affect the acceleration amplitude for both vehicle and turnout section. Generally, the acceleration amplitudes come to be smallest with train speed as 20 km/h, and the amplitudes become largest at train speed of 40 km/h at most cases and especially with train load as AW2, which is caused by the resonance of the turnout;

(2) The vertical Sperling indexes of the test vehicle under all tested operating conditions are less than 2.5 showing that the vehicle is in excellent stability;

(3) Resonance phenomena is more obvious at the F-rail of the short rail joint and continuous beam, and the resonance frequency is 24.2 Hz.

Funding

This work was supported in part by the Research Grants Council of the Hong Kong Special Administrative Region (SAR), China (Grant No.: R-5020-18); in part by the National Natural Science Foundation of China (Grant No.: U1934209, 52232013, and 52072269); in part by Wuyi University's Hong Kong and Macao Joint Research and Development Fund (Grants No.: 2019WGALH15 and 2019WGALH17); and in part by the Innovation and Technology Commission of Hong Kong SAR Government, China (Grant No.: K-BBY1).

Data Availability

The data supporting our research results are included within the article or supplementary material.

Conflicts of Interest

The authors declare no conflict of interest.

References

[1] "Overview of technology and development of maglev and hyperloop systems," National Academies, 2022, https://trid.trb.org/view/2075187.

[2] H. W. Lee, K. C. Kim, and J. Lee, "Review of maglev train technologies," *IEEE T. Magn.*, vol. 42, no. 7, pp. 1917-1925, 2006. https://doi.org/10.1109/TMAG.2006.875842.

[3] M. Li, S. Luo, W. Ma, C. Lei, T. Li, Q. Hu, X. Zhang, and Y. Han, "Experimental study on dynamic performance of medium and low speed maglev train-track-bridge system," *Int J. Rail Transp.*, vol. 9, no. 3,

pp. 232-255, 2021. https://doi.org/10.1080/23248378.2020.1798294.
[4] H. S. Han, B. H. Yim, N. J. Lee, Y. C. Hur, and S. S. Kim, “Effects of the guideway’s vibrational characteristics on the dynamics of a Maglev vehicle,” *Vehicle Syst. Dyn*., vol. 47, no. 3, pp. 309-324, 2009. https://doi.org/10.1080/00423110802054342.
[5] J. Li, D. Zhou, J. Li, G. Zhang, and P. Yu, “Modeling and simulation of CMS04 maglev train with active controller,” *J Cent. South Univ*., vol. 22, no. 4, pp. 1366-1377, 2015. https://doi.org/10.1007/s11771-015-2654-z.
[6] Y. B. Yang and J. D. Yau, “Vertical and pitching resonance of train cars moving over a series of simple beams,” *J. Sound Vib*., vol. 337, pp. 135-149, 2015. https://doi.org/10.1016/j.jsv.2014.10.024.
[7] J. Li, D. Fang, D. Zhang, Y. Cai, Q. Ni, and J. Li, “A practical control strategy for the maglev self-excited resonance suppression,” *Math. Probl. Eng.*, vol. 2016, Article ID: 8071938, 2016. https://doi.org/10.1155/2016/8071938.
[8] W. Zhai, C. Zhao, and C. Cai, "Dynamic simulation of the EMS maglev vehicle-guideway-controller coupling system," *In Maglev Conf.*, vol. 2004, pp. 567-574, 2004.
[9] K. Popp and W. Schiehlen, “Dynamics of magnetically levitated vehicles on flexible guideways,” *Vehicle Syst. Dyn.*, vol. 4, no. 2-3, pp. 195-199, 1975. https://doi.org/10.1080/00423117508968491.
[10] Y. Cai, S. S. Chen, D. M. Rote, and H. T. Coffey, “Vehicle/guideway interaction for high speed vehicles on a flexible guideway,” *J. Sound Vib*., vol. 175, no. 5, pp. 625-646, 1994. https://doi.org/10.1006/jsvi.1994.1350.
[11] Y. Cai, S. S. Chen, D. M. Rote, and H. T. Coffey, “Vehicle/guideway dynamic interaction in maglev systems,” *J. Dyn. Sys., Meas., Control*, vol. 118, no. 3, pp. 526-530, 1996. https://doi.org/10.1115/1.2801176.
[12] H. Tsunashima and M. Abe, “Static and dynamic performance of permanent magnet suspension for maglev transport vehicle,” *Vehicle Syst. Dyn*., vol. 29, no. 2, pp. 83-111, 1998. https://doi.org/10.1080/00423119808969368.
[13] J. S. Lee, S. D. Kwon, M. Y. Kim, and I. H. Yeo, “A parametric study on the dynamics of urban transit maglev vehicle running on flexible guideway bridges,” *J. Sound Vib*., vol. 328, no. 3, pp. 301-317, 2009. https://doi.org/10.1016/j.jsv.2009.08.010.
[14] X. J. Zheng, J. J. Wu, and Y. H. Zhou, “Numerical analysis on dynamic control of five-degree-of-freedom maglev vehicle moving on flexible guideways,” *J. Sound Vib*., vol. 235, no. 1, pp. 43-61, 2000. https://doi.org/10.1006/jsvi.1999.2911.
[15] J. D. Yau, “Vibration control of maglev vehicles traveling over a flexible guideway,” *J. Sound Vib*., vol. 321, no. 1, pp. 184-200, 2009. https://doi.org/10.1016/j.jsv.2008.09.030.
[16] C. F. Zhao and W. M. Zhai, “Maglev vehicle/guideway vertical random response and ride quality,” *Vehicle Syst. Dyn*., vol. 38, no. 3, pp. 185-210, 2002. https://doi.org/10.1076/vesd.38.3.185.8289.
[17] J. Shi, Q. Wei, and Y. Zhao, “Analysis of dynamic response of the high-speed EMS maglev vehicle/guideway coupling system with random irregularity,” *Vehicle Syst. Dyn*., vol. 45, no. 12, pp. 1077-1095, 2007. https://doi.org/10.1080/00423110601178441.
[18] N. Hägele and F. Dignath, “Vertical dynamics of the Maglev vehicle Transrapid,” *Multibody Syst. Dyn.*, vol. 21, no. 3, pp. 213-231, 2009. https://doi.org/10.1007/s11044-008-9136-0.
[19] S. Ren, A. Romeijn, and K. Klap, “Dynamic Simulation of the Maglev Vehicle/Guideway System,” *J. Bridge Eng.*, vol. 15, no. 3, pp. 269-278, 2010. https://doi.org/10.1061/(ASCE)BE.1943-5592.0000071.
[20] K. J. Kim, J. B. Han, H. S. Han, and S. J. Yang, “Coupled vibration analysis of Maglev vehicle-guideway while standing still or moving at low speeds,” *Vehicle Syst. Dyn*., vol. 53, no. 4, pp. 587-601, 2015. https://doi.org/10.1080/00423114.2015.1013039.
[21] D. J. Min, M. R. Jung, M. Y. Kim, and J. W. Kwark, “Dynamic interaction analysis of maglev-guideway system based on a 3D full vehicle model,” *Int J. Struct. Stab. Dyn*., vol. 17, no. 1, Article ID: 1750006, 2017. https://doi.org/10.1142/S0219455417500067.
[22] L. Zhang and J. Huang, “Dynamic interaction analysis of the high-speed maglev vehicle/guideway system based on a field measurement and model updating method,” *Eng. Struct*., vol. 180, pp. 1-17, 2019. https://doi.org/10.1016/j.engstruct.2018.11.031.
[23] J. D. Yau, “Response of a maglev vehicle moving on a series of guideways with differential settlement,” *J. Sound Vib.*, vol. 324, no. 3-5, pp. 816-831, 2009. https://doi.org/10.1016/j.jsv.2009.02.031.
[24] J. D. Yau, “Aerodynamic vibrations of a maglev vehicle running on flexible guideways under oncoming wind actions,” *J. Sound Vib*., vol. 329, no. 10, pp. 1743-1759, 2010. https://doi.org/10.1016/j.jsv.2009.11.039.
[25] J. B. Han, H. S. Han, S. S. Kim, S. J. Yang, and K. J. Kim, “Design and validation of a slender guideway for Maglev vehicle by simulation and experiment,” *Vehicle Syst. Dyn*., vol. 54, no. 3, pp. 370-385, 2016. https://doi.org/10.1080/00423114.2015.1137957.
[26] X. Li, D. Wang, D. Liu, L. Xin, and X. Zhang, “Dynamic analysis of the interactions between a low-to-medium-speed maglev train and a bridge: Field test results of two typical bridges,” *P. I. Mech. Eng. F. J. Rai.*, vol. 232, no. 7, pp. 2039-2059, 2018. https://doi.org/10.1177/0954409718758502.

[27] Z. L. Wang, Y. L. Xu, G. Q. Li, Y. B. Yang, S. W. Chen, and X. L. Zhang, "Modelling and validation of coupled high-speed maglev train-and-viaduct systems considering support flexibility," Vehicle Syst. Dyn., vol. 57, no. 2, pp. 161-191, 2019. https://doi.org/10.1080/00423114.2018.1450517.
[28] D. Wang, X. Li, Y. Wang, and Q. Hu, "Dynamic interaction of the low-to-medium speed maglev train and bridges with different deflection ratios: Experimental and numerical analyses," *Adv. Struct. Eng.*, vol. 23, no. 11, pp. 2399-2413, 2020. https://doi.org/10.1177/1369433220913367.
[29] M. Li, S. Luo, W. Ma, T. Li, D. Gao, and Z. Xu, "Experimental and numerical investigations of the dynamic responses of low and medium speed maglev train-track-bridge coupled system," *Vehicle Syst. Dyn.*, vol. 60, no. 5, pp. 1555-1578, 2022. https://doi.org/10.1080/00423114.2020.1864417.
[30] X. Liang, T. Jiang, Y. Hong, J. Zhang, M. Jiang, and Z. Wang, "Vibration response analysis of simply supported box girder bridge-maglev train in accelerated test of Changsha maglev express," *Adv. Mater. Sci. Eng.*, vol. 2020, Article ID: 9563747, 2020. https://doi.org/10.1155/2020/9563747.
[31] D. Wang, X. Li, L. Liang, and X. Qiu, "Dynamic interaction analysis of bridges induced by a low-to-medium-speed maglev train," *J. Vib. Control*, vol. 26, no. 21-22, pp. 2013-2025, 2020. https://doi.org/10.1177/1077546320910006.
[32] S. M. Wang, Y. Q. Ni, Y. G. Sun, Y. Lu, and Y. F. Duan, "Modelling dynamic interaction of maglev train-controller-rail-bridge system by vector mechanics," *J. Sound Vib.*, vol. 533, Article ID: 117023, 2022. https://doi.org/10.1016/j.jsv.2022.117023.
[33] D. Zhou, C. H. Hansen, L. Jie, and W. Chang, "Review of coupled vibration problems in EMS maglev vehicles," *Int J. Acoust. Vib.*, vol. 15, no. 1, pp. 10-23, 2010. https://doi.org/10.20855/ijav.2010.15.1255.
[34] D. Wang, X. Li, Y. Wang, and Q. Hu, "Dynamic interaction of the low-to-medium speed maglev train and bridges with different deflection ratios: Experimental and numerical analyses," *Adv. Struct. Eng.*, vol. 23, no. 11, pp. 2399-2413, 2020. https://doi.org/10.1177/1369433220913367.
[35] M. Li, D. Gao, T. Li, S. Luo, W. Ma, and X. Chen, "Experimental investigation on vibration characteristics of the medium-low-speed maglev vehicle-turnout coupled system," *Railway Eng. Sci.*, vol. 30, pp. 242-261, 2011. https://doi.org/10.1007/s40534-021-00266-7.
[36] M. Li, D. Gao, T. Li, S. Luo, W. Ma, X. Chen, and L. Tong, "Dynamic interaction of medium-low-speed maglev train running on the turnout made of steel structures," *Vehicle Syst. Dyn.*, vol. 61, no. 4, pp. 1129-1150, 2022. https://doi.org/10.1080/00423114.2022.2064757.
[37] "Medium and low speed magnetic levitation traffic design specification," CJJ/T262-2017, 2019.
[38] "Specification for dynamic performance assessment and testing verification of rolling stock," CJJ/T262-2017, 2019.